

Facile synthesis of reduced graphene oxide/ $\text{NH}_4\text{V}_3\text{O}_8$ with high capacity as a cathode material for lithium ion batteries

Lingjiang Kou, Liyun Cao , Jianfeng Huang, Jun Yang

School of Materials Science & Engineering, Shanxi University of Science and Technology, Xi'an 710021, People's Republic of China

✉ E-mail: 2644245930@qq.com

Published in Micro & Nano Letters; Received on 27th March 2017; Revised on 14th June 2017; Accepted on 23rd June 2017

Owing to low-electronic conductivity and long lithium ion diffusion path of $\text{NH}_4\text{V}_3\text{O}_8$ limit its application for lithium-ion batteries (LIBs). To overcome these limitation, a new nano-composites material of $\text{NH}_4\text{V}_3\text{O}_8$ -based have been successfully fabricated by a facial and environmental friendly approach, without the addition of any other template or surfactant. A facile hydrothermal route is employed to synthesised the reduced graphene oxide(rGO)/ $\text{NH}_4\text{V}_3\text{O}_8$ composites. Results show that the $\text{NH}_4\text{V}_3\text{O}_8$ nano-belt are well distributed on the surface of rGO nanosheets. The resulted rGO/ $\text{NH}_4\text{V}_3\text{O}_8$ nanocomposites exhibit a high capacity as a cathode material for LIBs in comparison with the bare $\text{NH}_4\text{V}_3\text{O}_8$. When used as cathode material for LIBs, it delivers a maximum discharge capacity of 253 mAhg^{-1} at 15 mAg^{-1} , 70 mAhg^{-1} larger than that of the pristine one. The enhanced electrochemical performance is attributed to the synergetic effects between $\text{NH}_4\text{V}_3\text{O}_8$ and rGO, such as increased conductivity and shortened lithium ion diffusion path.

1. Introduction: Energy is the indispensable materials foundation for the development of human-society, economic growth and livelihood improvement. In recent years, however, along with the depletion of resources and the aggravation of environmental pollution, human beings are facing a severe energy shortage crisis [1]. The battery as a kind of energy storage equipment plays an irreplaceable role in the energy utilisation. Rechargeable lithium-ion batteries (LIBs) attract people's interest because of its high energy density, long cycle life, no memory effect and environment friendly. Widely used in mobile phones, laptops, power tools, digital cameras and so on. Obviously, it is also most likely to be used on a large-scale application in the plug-in hybrid electric vehicles and all-electronic vehicles [2, 3]. Cathode material is a key material for lithium ion battery. The quality of cathode material not only has a direct impact on the battery performance, but also has important practical significance to reduce the cost of electric vehicle industry [4].

As a promising cathode material for LIBs, vanadium oxides and their derivatives have attracted tremendous attentions due to their easy synthesis, low cost, high capacity and good structural reversibility [5]. Recently, there have been many researchers reported ammonium vanadium with different morphologies such as $(\text{NH}_4)_2\text{V}_6\text{O}_{16}$ nanorods [6, 7], $\text{NH}_4\text{V}_3\text{O}_8$ nanorods [8, 9], $\text{NH}_4\text{V}_4\text{O}_{10}$ nanobelts [10, 11], $(\text{NH}_4)_{0.83}\text{Na}_{0.43}\text{V}_4\text{O}_{10}$ nanoplatelets [12] and $\text{NH}_4\text{V}_3\text{O}_8$ /carbon nanotubes [13]. These efforts improve the electrochemical lithium insertion performances of ammonium vanadate significantly. Nevertheless, the above mentioned materials need a time longer than 24 h, high temperature or surfactant assist. Owing to poor conductivity of the $\text{NH}_4\text{V}_3\text{O}_8$, which would influence the rapid transferring of Li^+ and e^- , cause a low-rate capability.

Graphene, a high-theoretical surface area of $2630 \text{ m}^2/\text{g}$, with great electrical conductivity and excellent mechanical electrochemical stability. Commonly introduced as matrices to buffer the volume changes and enhance the structural stability [14]. Graphene-modified V_2O_5 [15], Li_3VO_4 [16] and LiFePO_4 [17] has been prepared, which will much improved the specific capacity. To the best of our knowledge there has been no report on the composite of $\text{NH}_4\text{V}_3\text{O}_8$ nanorods grafted onto graphene. Herein, a facile hydrothermal approach is introduced for growing one-dimensional $\text{NH}_4\text{V}_3\text{O}_8$ nano-belt on graphene sheets.

2. Experimental: Synthesis of rGO/ $\text{NH}_4\text{V}_3\text{O}_8$: all chemicals in our experiment were analytical grade and used directly without any purification. In a typical experiment, 30 mg graphene oxide was suspended in 60 mg deionised water with dispersion by ultrasonication. Then NH_4VO_3 (0.20g) was dissolved in deionised water successively to form a light-yellow solution. After that, a proper amount of hydrochloric acid was further added drop-wise into the above-obtained solution under continuous stirring. Adjust the pH value of the solution and resulting wine-coloured solution. Finally, the resulting mixed solution was transferred into a 100 mL Teflon-lined stainless steel autoclave. The autoclave was sealed and heated at 150°C for 6 h and then cooled to room temperature naturally. The precipitate was collected by centrifugation, wash with deionised water and ethanol for several times. The final rGO/ $\text{NH}_4\text{V}_3\text{O}_8$ composites were obtained after drying at 60°C overnight.

Characterisation: The phase composition of the sample was studied by an X-ray diffractometer (XRD, Rigaku, Japan, D/max-2200) with Cu $K\alpha$ radiation ($\lambda = 0.15406 \text{ nm}$). The morphology of the products was observed by field emission scanning electron microscopy (SEM) (S4800, Hitachi, Japan) at an acceleration voltage of 3 KV. Different scanning calorimetry and thermal gravimetry (DSC/TG) for sample was carried out with a NETZSCH STA 449F3 differential scanning calorimeter under air atmosphere at a ramping rate of $10^\circ\text{C min}^{-1}$.

Electrochemical measurements: The electrochemical measurements were performed using CR2032 coin-type cells, consisting of the cathode and a lithium metal anode, separated by a porous polyethylene film (Celgard 2400) and electrolyte (1 M LiPF_6 in ethylene carbonate and dimethyl carbonate (1:1 in the volume)). The working electrodes were prepared from a mixture of rGO/ NH_4VO_3 powder, acetylene black and polyvinylidene fluoride binder were mixed together in a ratio of 80:10:10 in a solvent of N-methyl-2-pyrrolidone to form a homogenous slurry and pasted on pure aluminium foil. The cells were constructed in an Ar-filled glovebox and then cycled galvanostatically between 1.5 and 4.0 V with a multichannel battery testing system (Shenzhen, Neware, China). Cyclic voltammograms (CV) were performed by a CHI660E electrochemical station (Hanghai, Chenhua, Chian). All the tests were recorded at room temperature.

3. Results and discussion: The XRD pattern of the as-synthesised products is shown in Fig. 1. All diffraction peaks in XRD pattern could be readily indexed to a monoclinic crystalline $\text{NH}_4\text{V}_3\text{O}_8$ phase (JCPDS Card No. 881473, space group $\text{P}2_1/\text{m}$). The lattice parameters $a = 0.7850 \text{ nm}$, $b = 0.8405 \text{ nm}$, $c = 0.4989 \text{ nm}$ and $\beta = 96.39^\circ$. As seen, no other phases have been detected, showing that the products are of high purity. Obviously, as observed, the $\text{NH}_4\text{V}_3\text{O}_8$ without GO of diffraction peak (001) is much higher than that $\text{rGO}/\text{NH}_4\text{V}_3\text{O}_8$. It is generally known that the higher the relative intensity of diffraction peak (001), the better the degree of crystallinity. Fortunately, the poor ordering of crystal is conducive to the diffusion of Li^+ intercalation and de-intercalation and it would lead to a short Li^+ diffusion path. Therefore, the relatively low intensity of diffraction peak (001) of $\text{NH}_4\text{V}_3\text{O}_8$ with GO will affect the electrochemical properties of the material [18, 19].

Fig. 2 shows SEM of the $\text{NH}_4\text{V}_3\text{O}_8$ and $\text{rGO}/\text{NH}_4\text{V}_3\text{O}_8$ composite. As can be seen, the morphology of the $\text{NH}_4\text{V}_3\text{O}_8$ (Figs. 2a and b) is 1D nano-belt. The belts have the width of 20–30 nm and the length of 0.8–1 μm . However, the agglomeration of the nano-belt is serious. The $\text{NH}_4\text{V}_3\text{O}_8$ nanoparticles were irregular with the belt growth direction. As for the as-prepared $\text{rGO}/\text{NH}_4\text{V}_3\text{O}_8$ nanocomposites, the overall morphologies were shown in Fig. 2c. It can be seen that graphene nanosheets were, on the whole, even in combination with $\text{NH}_4\text{V}_3\text{O}_8$ nanoparticles.

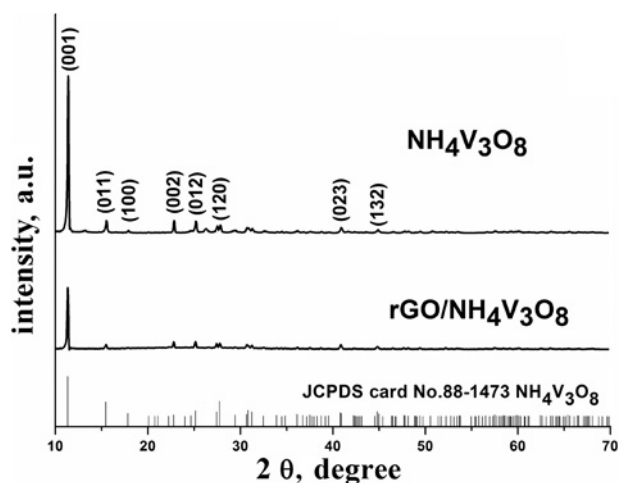


Fig. 1 X-ray diffraction pattern of the as-prepared materials

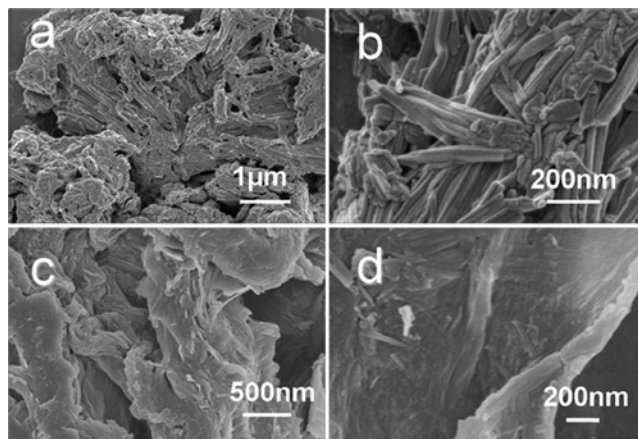


Fig. 2 SEM images of the as-prepared $\text{NH}_4\text{V}_3\text{O}_8$ a, b and $\text{rGO}/\text{NH}_4\text{V}_3\text{O}_8$ c, d

The enlarged morphological image (Fig. 2d) further reveals that the $\text{NH}_4\text{V}_3\text{O}_8$ nano-belt were well distributed on the rGO nanosheets. This kind of good distribution way can increase the contact area electrolyte and $\text{rGO}/\text{NH}_4\text{V}_3\text{O}_8$ electrode material, which will increase the electrochemical properties [20].

To determine the weight percentage of rGO in $\text{rGO}/\text{NH}_4\text{V}_3\text{O}_8$ nanocomposites, DSC-TG test for $\text{rGO}/\text{NH}_4\text{V}_3\text{O}_8$ were carried out in air. As shown in Fig. 3, the weight loss of 2.49 wt% below the temperature of 300°C is attributed to the evaporation of moisture, contain the physically absorbed or chemisorbed water molecules. At 320°C ammonium vanadium transformed into nonstoichiometric V_2O_5 . The thermal decomposition of graphene occurred mainly in the $400\text{--}600^\circ\text{C}$, leading to a weight loss of 12.4 wt%. Even further, the DSC curves also shows an endothermic peak looked at 670°C might be the cause of the melting of V_2O_5 . Therefore, removing the weight of moisture, the final weight percentage of graphene was determined to be $\sim 12.4 \text{ wt\%}$ in the composite.

The first three cycles cyclic voltammogram of the as-prepared $\text{rGO}/\text{NH}_4\text{V}_3\text{O}_8$ at a scan rate of 0.1 mV s^{-1} in $1.5\text{--}4.0 \text{ V}$ are shown in Fig. 4. The oxidation and reduction peaks correspond to the delithiation and lithiation processes of the host material. There are two obvious pairs of redox peaks, with the oxidation peaks at 1.9 and 3.2 V and the corresponding reduction peaks at 2.8 and 2.4 V , which indicated a multi-step lithiation process. It is obvious that the third cycle has a higher redox peak than the first

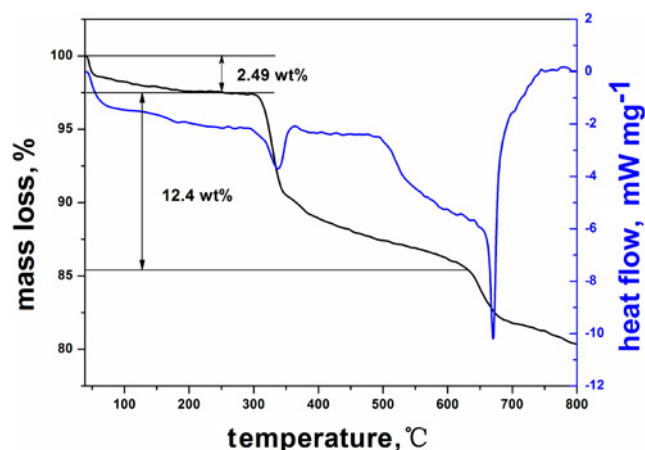


Fig. 3 DSC-TG curves of the prepared $\text{rGO}/\text{NH}_4\text{V}_3\text{O}_8$ nanocomposites

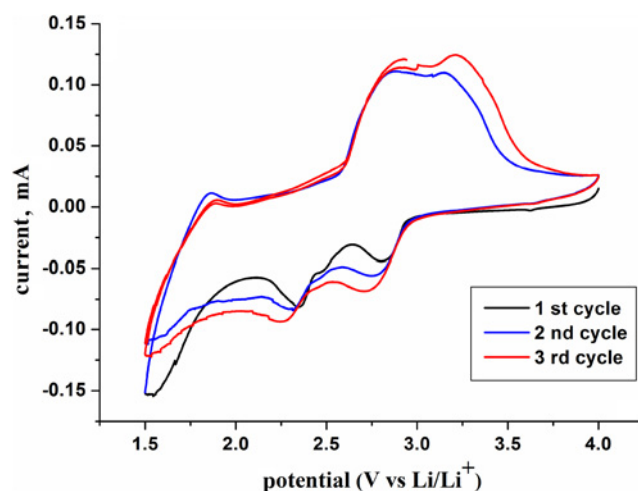


Fig. 4 First three CV cycle curves of the as-prepared $\text{rGO}/\text{NH}_4\text{V}_3\text{O}_8$ between 1.5 and 4 V at a scan rate of 0.1 mV s^{-1}

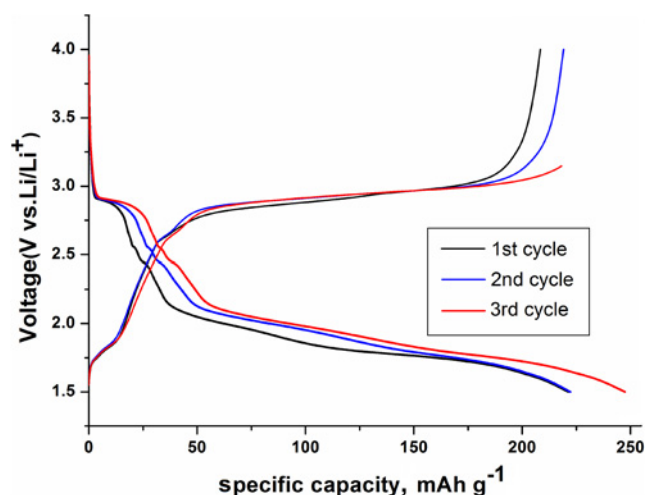


Fig. 5 Typical charge/discharge curves of $\text{rGO}/\text{NH}_4\text{V}_3\text{O}_8$ at 15 mA g^{-1}

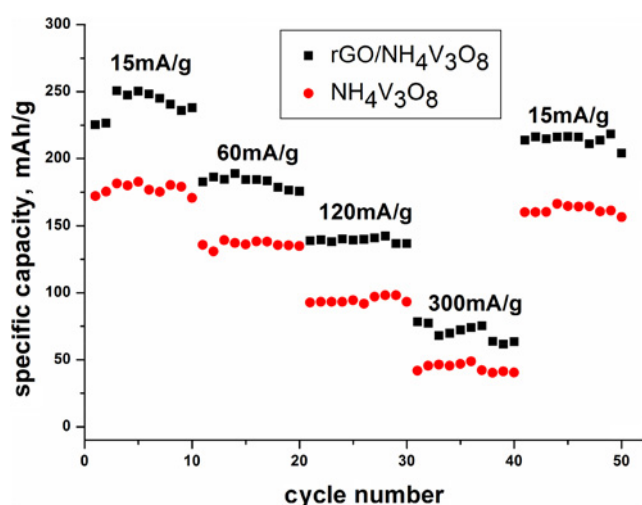


Fig. 6 Capacity performance at various cycling rates of the as-prepared $\text{NH}_4\text{V}_3\text{O}_8$ and $\text{rGO}/\text{NH}_4\text{V}_3\text{O}_8$ nanocomposites

two cycles, suggesting that the first few cycles has a higher capacity and a faster kinetic for Li^+ intercalation/de-intercalation. And this is consistent with the results of charge/discharge test.

The performance of Li^+ insertion/extraction of $\text{rGO}/\text{NH}_4\text{V}_3\text{O}_8$ nanocomposites as a cathode material was studied by galvanostatic charge-discharge measurements. Fig. 5 shows the first three charge/discharge curves of $\text{rGO}/\text{NH}_4\text{V}_3\text{O}_8$ electrodes in the voltage window of 1.5–4.0 V vs. Li^+/Li at a current density of 15 mA g^{-1} . As observed, the first three cycle curves show similar shape and two discharge voltage plateaus at 2.8 and 1.7 V. At the beginning of the discharge process, voltage rapidly degradation from 4.0 to 2.9 V. Soon afterwards, the discharge capacity continues to grow with the decrease of voltage in the potential range of 2.9–2.8 and 2.0–1.7 V.

Fig. 6 shows the rate capability of bare $\text{NH}_4\text{V}_3\text{O}_8$ and $\text{rGO}/\text{NH}_4\text{V}_3\text{O}_8$ composite electrodes at various current densities from 15 to 300 mA g^{-1} . As the current density increases, the capacity is expected to decrease, which is the result of a reduction in the utilisation of the electrode material. At 15, 60, 120, 300 mA g^{-1} , the maximum discharge capacity of $\text{rGO}/\text{NH}_4\text{V}_3\text{O}_8$ is 253, 181, 148 and 79 mAh g^{-1} , respectively. While that of $\text{NH}_4\text{V}_3\text{O}_8$ decreases to 183, 142, 101 and 50 mAh g^{-1} . Obviously, the $\text{rGO}/\text{NH}_4\text{V}_3\text{O}_8$ composite delivers higher discharge capacity than the $\text{NH}_4\text{V}_3\text{O}_8$ at all tested current densities, which can be attributed to the rGO

with high-specific surface area, high electron mobility, good chemical stability, short diffusion distance and freedom for volume change [21].

4. Conclusions: In summary, we successfully fabricated a $\text{rGO}/\text{NH}_4\text{V}_3\text{O}_8$ nanocomposites through a facile hydrothermal route. The $\text{NH}_4\text{V}_3\text{O}_8$ nanobelts are anchored to graphene nanosheets through coordination effect. Compared with the $\text{NH}_4\text{V}_3\text{O}_8$, the $\text{rGO}/\text{NH}_4\text{V}_3\text{O}_8$ revealed an improvement in electrochemical performance of the lithium ion battery, shown by highly reversible capacities and good rate capabilities. This good electrochemical performance is attributed to the nanosized one-dimensional $\text{NH}_4\text{V}_3\text{O}_8$ homogeneous grown on rGO. The rGO and The unique composite structure leads to high Li^+ diffusion coefficient and a good structural stability during the electrochemical process. This work on graphene nanosheets as the carbon matrix in a composite material could be extended to other vanadates.

5. Acknowledgements: This work was supported by the National Natural Science Foundation of China (grant no. 51102196), the science and technology project of the young star of Shaanxi Province (grant no. 2014KJXX-68), the Innovation Team Assistance Foundation of Shaanxi Province (grant no. 2013KCT-06) and the scientific research project of Shaanxi education department (grant no. 14Jk1104). Their supports are gratefully acknowledged.

6 References

- [1] Qureshi M.I., Rasli A.M., Zaman K.: 'Energy crisis, greenhouse gas emissions and sectoral growth reforms: repairing the fabricated mosaic', *J. Clean Prod.*, 2016, **112**, pp. 3657–3666
- [2] Lee H., Yanilmaz M., Toprakci O., ET AL.: 'A review of recent developments in membrane separators for rechargeable lithium-ion batteries', *Energy Environ. Sci.*, 2014, **7**, (12), pp. 3857–3886
- [3] Hayner C.M., Zhao X., Kung H.H.: 'Materials for rechargeable lithium-ion batteries', *Ann. Rev. Chem. Biomol. Eng.*, 2012, **3**, p. 445
- [4] Xu X., Luo Y.-Z., Mai L.-Q., ET AL.: 'Topotactically synthesized ultralong LiV_3O_8 nanowire cathode materials for high-rate and long-life rechargeable lithium batteries', *NPG Asia Mater.*, 2012, **4**, (6), p. e20
- [5] Li N., Huang W., Shi Q., ET AL.: 'A CTAB-assisted hydrothermal synthesis of $\text{VO}_2(\text{B})$ nanostructures for lithium-ion battery application', *Ceram. Int.*, 2013, **39**, (6), pp. 6199–6206
- [6] Chithaiah P., Vijaya kumar G., Nagabhushana G.P., ET AL.: 'Synthesis of single crystalline $(\text{NH}_4)_2\text{V}_6\text{O}_{16} \cdot 1.5\text{H}_2\text{O}$ nest-like structures', *Phys. E: Low-Dimen. Syst. Nanostructures*, 2014, **59**, pp. 218–222
- [7] Fei H., Wu X., Li H., ET AL.: 'Novel sodium intercalated $(\text{NH}_4)_2\text{V}_6\text{O}_{16}$ platelets: High performance cathode materials for lithium-ion battery', *J. Colloid Interface Sci.*, 2014, **415**, pp. 85–88
- [8] Ottmann A., Zakharova G.S., Ehrstein B., ET AL.: 'Electrochemical performance of single crystal belt-like $\text{NH}_4\text{V}_3\text{O}_8$ as cathode material for lithium-ion batteries', *Electrochim. Acta*, 2015, **174**, pp. 682–687
- [9] Cao S., Huang J., Cheng Y., ET AL.: 'Facile synthesis of ultralong $\text{NH}_4\text{V}_3\text{O}_8$ nanobelts cathode material for lithium ion battery', *J. Electroanal. Chem.*, 2015, **752**, pp. 12–16
- [10] Abbood H.A., Peng H., Gao X., ET AL.: 'Fabrication of cross-like $\text{NH}_4\text{V}_4\text{O}_{10}$ nanobelt array controlled by CMC as soft template and photocatalytic activity of its calcinated product', *Chem. Eng. J.*, 2012, **209**, pp. 245–254
- [11] Sarkar S., Veluri P.S., Mitra S.: 'Morphology controlled synthesis of layered $\text{NH}_4\text{V}_4\text{O}_{10}$ and the impact of binder on stable high rate electrochemical performance', *Electrochim. Acta*, 2014, **132**, pp. 448–456
- [12] Fei H., Shen Z., Wang J., ET AL.: 'Flower-like $(\text{NH}_4)_{0.83}\text{Na}_{0.43}\text{V}_4\text{O}_{10} \cdot 0.26\text{H}_2\text{O}$ nano-structure for stable lithium battery electrodes', *J. Power Sources*, 2009, **189**, (2), pp. 1164–1166
- [13] Wang H., Huang K., Ren Y., ET AL.: ' $\text{NH}_4\text{V}_3\text{O}_8$ /carbon nanotubes composite cathode material with high capacity and good rate capability', *J. Power Sources*, 2011, **196**, (22), pp. 9786–9791
- [14] Kucinskis G., Bajars G., Kleperis J.: 'Graphene in lithium ion battery cathode materials: A review', *J. Power Sources*, 2013, **240**, p. 66

- [15] Liu Y., Wang Y., Zhang Y., *ET AL.*: 'Controllable preparation of V₂O₅/graphene nanocomposites as cathode materials for lithium-ion batteries', *Nanoscale Res. Lett.*, 2016, **11**, (1), p. 549
- [16] Liu J., Lu P.-J., Liang S., *ET AL.*: 'Ultrathin Li₃VO₄ nanoribbon/graphene sandwich-like nanostructures with ultrahigh lithium ion storage properties', *Nano Energy*, 2015, **12**, pp. 709–724
- [17] Lung-Hao Hu B., Wu F.-Y., Lin C.-T., *ET AL.*: 'Graphene-modified LiFePO₄ cathode for lithium ion battery beyond theoretical capacity', *Nature Commun.*, 2013, **4**, p. 1687
- [18] Wang H., Huang K., Liu S., *ET AL.*: 'Electrochemical property of NH₄V₃O₈·0.2H₂O flakes prepared by surfactant assisted hydrothermal method', *J. Power Sources*, 2011, **196**, (2), pp. 788–792
- [19] Wang H., Ren Y., Wang W., *ET AL.*: 'NH₄V₃O₈ nanorod as a high performance cathode material for rechargeable Li-ion batteries', *J. Power Sources*, 2012, **199**, pp. 315–321
- [20] Shanshan C., Jianfeng H., Zhanwei X., *ET AL.*: 'Influence of microwave heating on the structure and electrochemical property of NH₄V₃O₈ cathode material for lithium ion batteries', *Ceramics Int.*, 2015, **41**, (5), pp. 6747–6752
- [21] Chen D., Yi R., Chen S., *ET AL.*: 'Solvothermal synthesis of V₂O₅/graphene nanocomposites for high performance lithium ion batteries', *Mater. Sci. Eng.: B*, 2014, **185**, pp. 7–12